

Anti-Correlated Cortical Networks of Intrinsic Connectivity in the Rat Brain

Adam J. Schwarz,^{1,2} Natalia Gass,³ Alexander Sartorius,^{3,4} Celine Risterucci,⁵ Michael Spedding,⁶ Esther Schenker,⁶ Andreas Meyer-Lindenberg,⁴ and Wolfgang Weber-Fahr³

Abstract

In humans, resting-state blood oxygen level-dependent (BOLD) signals in the default mode network (DMN) are temporally anti-correlated with those from a lateral cortical network involving the frontal eye fields, secondary somatosensory and posterior insular cortices. Here, we demonstrate the existence of an analogous lateral cortical network in the rat brain, extending laterally from anterior secondary sensorimotor regions to the insular cortex and exhibiting low-frequency BOLD fluctuations that are temporally anti-correlated with a midline “DMN-like” network comprising posterior/anterior cingulate and prefrontal cortices. The primary nexus for this anti-correlation relationship was the anterior secondary motor cortex, close to regions that have been identified with frontal eye fields in the rat brain. The anti-correlation relationship was corroborated after global signal removal, underscoring this finding as a robust property of the functional connectivity signature in the rat brain. These anti-correlated networks demonstrate strong anatomical homology to networks identified in human and monkey connectivity studies, extend the known preserved functional connectivity relationships between rodent and primates, and support the use of resting-state functional magnetic resonance imaging as a translational imaging method between rat models and humans.

Key words: anti-correlated; brain; fMRI; functional connectivity; networks; rat

Introduction

FUNCTIONAL IMAGING STUDIES have revealed a system-level structure of functional connectivity in the human brain, comprising distinguishable networks of brain regions. This phenomenon is most commonly observed via temporal correlations of low-frequency blood oxygen level-dependent (BOLD) signal fluctuations (Biswal et al., 1995). The basic nature and relationship between the major networks, most often studied in the absence of an explicit task (i.e., in the “resting state”), is now well established in humans (Beckmann et al., 2005; Fox et al., 2005; Fox and Raichle, 2007; Raichle, 2011), and similar patterns of functional coupling have been observed in nonhuman primates (Hutchison and Everling, 2012; Vincent et al., 2007).

One network that has been the subject of particular interest is the so-called “default mode” network (DMN), which links regions in the posterior cingulate/precuneus and medial pre-

frontal cortex (PFC) to lateral parietal and prefrontal regions (Raichle et al., 2001). Resting-state BOLD signals within this network are temporally anti-correlated with those from other cortical networks comprising regions that are typically activated in tasks requiring cognitive control and attention, including the intraparietal sulci, supplementary motor area, and precentral gyrus extending toward the insula (Chai et al., 2012; Fox et al., 2005; Whitfield-Gabrieli and Nieto-Castanon, 2012).

Recently, plausible correlation patterns from low-frequency BOLD oscillations have begun to be elucidated in the rat brain (Gass et al., 2013; Jonckers et al., 2011; Lu et al., 2012; Nasrallah et al., 2012; Pawela et al., 2008; Upadhyay et al., 2011; Zhang et al., 2010), and anti-correlation relationships have begun to be observed (Liang et al., 2012). However, the degree to which anti-correlated systems exist within the rat cortex, and their homology to established networks in primate species, has yet to be fully elucidated. In

¹Lilly Research Laboratories, Eli Lilly and Company, Indianapolis, Indiana.

²Department of Psychological and Brain Sciences, Indiana University, Bloomington, Indiana.

Departments of ³Neuroimaging and ⁴Psychiatry and Psychotherapy, Central Institute of Mental Health, Medical Faculty Mannheim, University of Heidelberg, Mannheim, Germany.

⁵F. Hoffmann-La Roche Ltd, Pharmaceuticals Division CNS Biomarkers, Basel, Switzerland.

⁶Instituts de Recherches Servier, Croissy s/Seine, France.

this article, we present evidence from BOLD resting-state functional magnetic resonance imaging (rsfMRI) for the existence of anti-correlated intrinsic connectivity networks in the rat cortex where, in homology to humans, the midline anterior-posterior cingulate/PFC network is anti-correlated with a lateral cortical network involving the anterior lateral sensorimotor cortices and extending to the insula.

Methods

Animals and experimental procedures

MRI experiments were performed on 16 Sprague–Dawley male rats (weight 340–392 g, age 2–3 months). All procedures fulfilled the regulations covering animal experimentation within the European Union (European Communities Council Directive 86/609/EEC) and Germany (Deutsches Tierschutzgesetz). Experiments were approved by the German animal welfare authorities (Regierungspräsidium Karlsruhe) and conducted at the Central Institute of Mental Health in Mannheim, Germany.

Rats were initially anesthetized with 4% isoflurane in a mix of 70% N₂/30% O₂; after positioning in the scanner (head first, prone), anesthesia was maintained at ~2.5% for adjustments. After completion of these, a bolus of 0.5 ml (0.07 mg/kg) medetomidine solution (Domitor[®]; Janssen-Cilag) was subcutaneously injected. Isoflurane was slowly discontinued within the next 10 min, and a continuous infusion of 1 ml/h (0.14 mg/kg/h) medetomidine solution began. After completion of each experiment, Atipamezol (Antisedan; Janssen-Cilag) was subcutaneously injected (1 mg/kg) along with ~2 ml of saline to reverse the sedative effect and compensate the fluid loss during the experiment.

Breathing and cardiac rates, as well as blood oxygen levels and the body temperature were monitored continually while the animals were in the scanner. Respiratory and cardiac signals were recorded (10 ms resolution) using a signal breakout module and a signal recorder (Small Animal Instruments, Inc.). Breathing rates under medetomidine remained within the range of 50–100 breaths per minute, the cardiac rate remained within 190–280 beats per minute, and blood oxygenation levels during the resting-state measurements were in the range 80–100%. To provide an additional control over the body temperature, circulation of warm water was supplied along the lower part of the animal body.

Image data acquisition

All experiments were performed on a 94/20 Bruker Biospec MRI scanner (9.4 T; Bruker BioSpec) with Avance III hardware, BGA12S gradients system with a maximum strength of 30042 Hz/mm, and running Paravision 5.1 software. A linear transmitter coil combined with rat brain linear receive-only coil array were used for radiofrequency transmission and reception, respectively. rsfMRI data were acquired using an echo planar imaging (EPI) sequence with the following parameters: TR/TE 1700/17.5 ms, flip angle 60°, 1 segment, 1 average, 29 coronal slices, 96×96 matrix, field of view (35×35) mm², slice thickness of 0.5 mm with 0.2 mm inter-slice gap, in-plane voxel dimension of 0.36 mm, and 300 volumes for an acquisition time of 8.5 min. To enable correction of EPI geometric distortion in postprocessing, a field map was also acquired (TR 20 ms, TE (dual echo) 1.7/5.7 ms, flip angle 20°, 64×64×64 matrix).

Image data postprocessing

The image time series data were postprocessed using tools from SPM8 (www.fil.ion.ucl.ac.uk/spm/software/spm8/) (Ashburner, 2011), FMRIB Software Library (FSL, v.4.1; www.fmrib.ox.ac.uk/fsl) (Jenkinson et al., 2012), and Analysis of Functional Neuroimages (AFNI, v. 2011_12_21_1014; <http://afni.nimh.nih.gov>) (Cox, 2012). First, the EPI data were realigned (motion correction) and unwrapped (correction for geometric distortions due to magnetic field inhomogeneities) (FieldMap toolbox; statistical parametric mapping [SPM]). Second, the head motion traces were regressed from the data using the *fsl_regfilt* utility (FSL). Third, physiological noise (respiratory and cardiac signals) were regressed from the time series using the RETROICOR retrospective correction technique (Glover et al., 2000) as implemented in the Aztec toolbox (van Buuren et al., 2009). Data were then corrected for slice timing offsets (SPM).

The resulting filtered time series were spatially normalized to a rat brain template with co-registered anatomical atlas (v6) positioned in the Paxinos and Watson stereotactic coordinate system (Schwarz et al., 2006). This was performed in two steps: (1) linear co-registration (six degree-of-freedom rigid-body transformation) to the template, followed by (2) nonlinear normalization (SPM). The normalised data had a spatial resolution of 0.2×0.2×0.8 mm³ (96×96×30 matrix). To evaluate the additional effect of global signal removal, versions of the time series with the whole-brain average time course regressed out (AFNI) were also computed. Finally, the image time series were band-pass filtered to a frequency window of 0.01–0.1 Hz (AFNI) and spatially smoothed using a Gaussian kernel of full width at half maximum of 0.6 mm.

Seed locations are reported in stereotactic coordinates of Paxinos and Watson (Paxinos and Watson, 1998) as medial-lateral (M-L), dorsal-ventral (D-V), and anterior-posterior (A-P) relative to bregma. We also follow Paxinos nomenclature for individual atlas structures.

Connectivity analyses

Small seed regions of 3×3×1 voxels (0.6×0.6×0.8 mm) were specified so as to specifically sample (1) three midline retrosplenial, cingulate, and medial PFC locations within the “DMN-like” regions of the hippocampal-prefrontal network previously identified (s02, s08, and s12) from (Schwarz et al., 2013); and (2) three bilateral seed locations within a lateral secondary sensorimotor/insula network, denoted λ 01, λ 02, and λ 03 (see Table 1 and Fig. 1). Seed λ 01 was identified on the basis of the anti-correlations with the midline cingulate/prefrontal network previously observed (Schwarz et al., 2013), and is slightly anterior to the anterior cortical seed c01 used in that paper. Seeds λ 02 and λ 03 were then specified to assess the connectivity patterns associated with more posterior locations within the network positively correlated with λ 01.

Mean time courses from each seed were calculated, and direct inter-seed connectivity relationships were assessed using the Pearson product-moment correlation coefficient as an index of similarity between all pairs of seeds. The group-level significance of each ROI-ROI (anti-) correlation relationship was assessed using one-sample *t*-tests on *z*-transformed versions of the correlation coefficients (using Fisher's *r*-to-*z*

TABLE 1. DEFINITION OF SEED REGIONS OF INTEREST

Seed	Brain region (atlas structure)	Stereotaxic coordinates of ROI centers (relative to bregma)		
		M-L (mm)	A-V (mm)	A-P (mm)
Midline prefrontal/cingulate network				
s02	Medial prefrontal cortex (PrL)	0.0	2.7	4.0
s08	Anterior cingulate cortex (Cg1)	0.0	-1.6	1.6
s12	Retrosplenial cortex (RSGb)	0.0	1.4	-4.0
Lateral secondary cortical network				
l01	Anterior secondary motor cortex (M2)	±3.7	2.5	4.0
l02	Primary somatosensory cortex, jaw region (SIJ)	±5.3	3.9	1.6
l03	Insular cortex (Ins)	±6.4	6.2	-0.8

See also Figure 1.
ROI, regions of interest.

transform). Similarly, differences in ROI-ROI correlation coefficients between nonglobally corrected and globally corrected processing were assessed quantitatively using paired *t*-tests on the *z*-transformed correlation coefficients. For each of the nonglobally corrected region of interest (ROI) pairs, the globally corrected ROI pairs, and the comparison between them, the tests were corrected for multiple comparisons using the Benjamini–Hochberg method and a false discovery rate of 0.05.

To map the connectivity relationships at a higher spatial resolution, each seed was also used to generate a whole-brain correlation map, using the mean time course from the seed as a regressor for each voxel (AFNI). Individual subject correlation maps were transformed to normally-distributed *z* scores using Fisher's *r*-to-*z* transformation before assessing consistent group level connectivity distributions using one

sample *t*-tests. Resulting group maps were thresholded at $|T| > 2.9$, followed by a cluster-level multiple comparison correction at a significance level of $p < 0.05$ (FSL). 3D surface renderings were generated using Caret (<http://brainvis.wustl.edu/wiki/index.php/Caret>About>).

Results

The correlation map referenced to seed l01, in the anterior secondary motor cortex, revealed two distinct, anti-correlated cortical networks (Fig. 2). This seed was positively correlated with a network comprising lateral cortical brain structures, extending bilaterally from the secondary motor cortex anteriorly back through secondary sensory cortex and the insula, and anti-correlated with midline prefrontal, cingulate, and mediadorsal cortical areas.

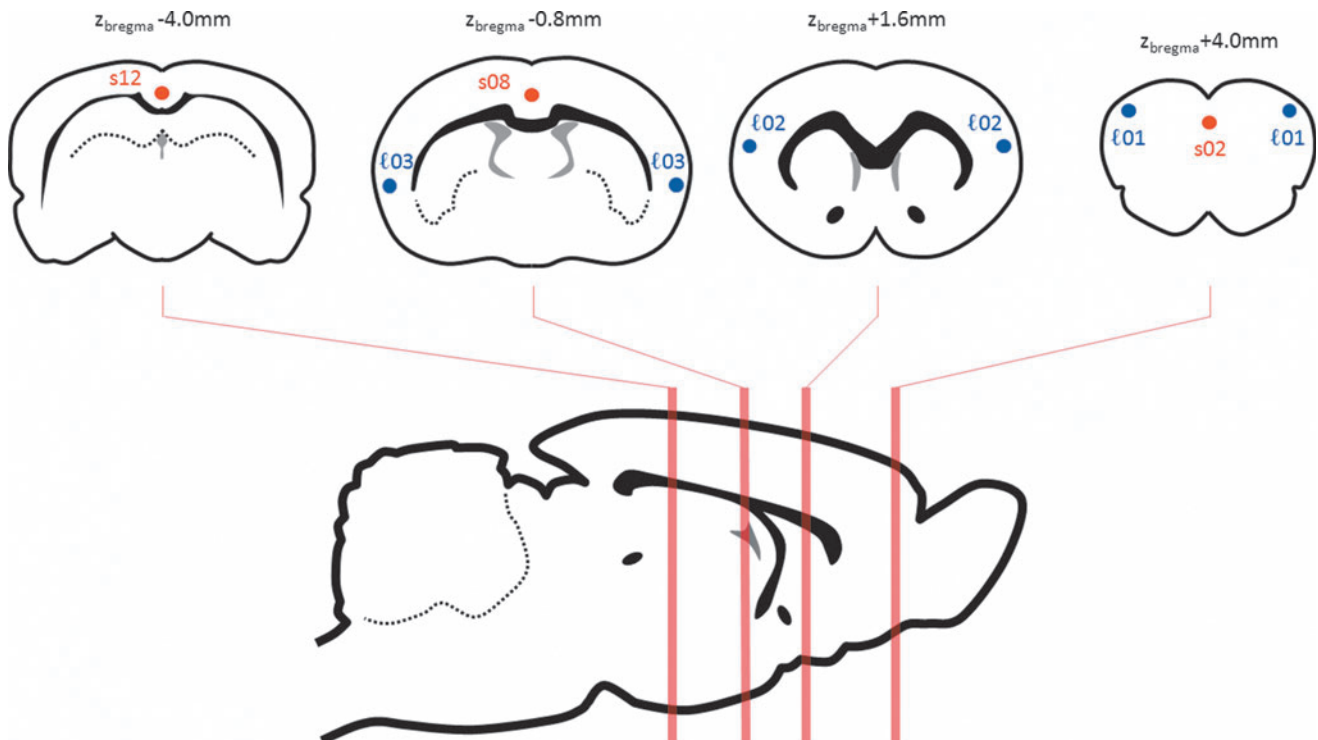


FIG. 1. Schematic location of seeds (see also Table 1).

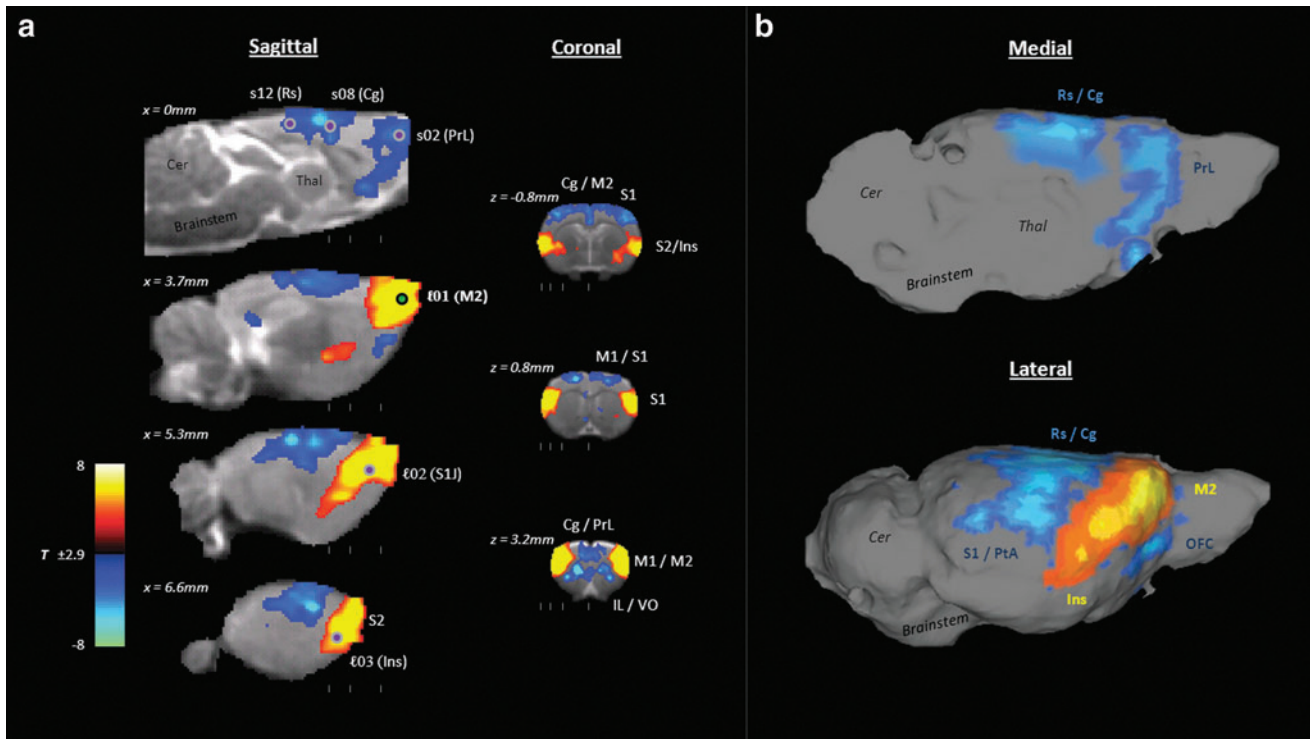


FIG. 2. Seed correlation map for seed $\ell 01$ (anterior motor cortex), showing the anti-correlation relationship between the lateral secondary cortical network (red) and more midline structures, including the cingulate and medial prefrontal cortices (blue). **(a)** Sagittal and coronal slices of networks overlaid on T_2 -weighted anatomical template image. Vertical gray dashes below the images indicate the location of the orthogonal slices shown. The green dot denotes the location of the seed ($\ell 01$) of this map; the purple dots indicate the location of the other seeds studied in this paper. **(b)** Medial and lateral views of the anti-correlated networks ($\ell 01$ seed) projected onto surface reconstruction of rat brain.

Analysis of ROI-to-ROI coupling between seed pairs confirmed this relationship (Fig. 3, see also Supplementary Table S1; Supplementary Data are available online at www.liebertpub.com/brain). The strongest correlations were observed between seeds in the lateral cortical network. Regions within the two different networks were anti-correlated across networks, with the strongest negative correlation observed between the anterior seeds within each network.

Seed $\ell 01$ was the primary nexus for the anti-correlation relationship, delineating both the lateral cortical network and the midline prefrontal/cingulate networks. Other seeds within these two networks elicited more focal anti-correlations in seed connectivity maps, consistent with a general weakening of the anti-correlation strength for more posterior seeds (Fig. 4). The lateral network was anatomically well-delimited, with the neuroanatomical distributions of the positive correlations from each of the three seeds therein ($\ell 01$, $\ell 02$ and $\ell 03$) substantially overlapping. These distinct networks reveal a functional dissociation within the rat sensorimotor and parietal cortices, with more mediadorsal regions closely coupled to the midline PFC/cingulate network; whereas the more anterior lateral and ventrolateral cortical areas are associated with the lateral cortical network.

These anti-correlation relationships were largely maintained if a global signal correction was applied. At the ROI level, the correlations within the lateral network were unchanged, and the anti-correlations between networks were similar (only $\ell 03$ - $s02$ was more strongly anti-correlated, $p < 0.01$) after global signal regression (Fig. 3). The most prom-

inent effects of global signal correction were reduced correlation strengths within the midline cingulate/PFC network ($p < 0.001$ for all three ROI pairs). These effects were also evident in seed correlation maps, where the positive correlations within the lateral network were almost identical to those observed in the absence of global signal removal, and maintained strong anti-correlations with regions in the midline network; whereas the inter-correlations within the midline cingulate/PFC network itself were more focal, both laterally and antero-posteriorly (Fig. 5).

Discussion

We demonstrated the presence of anti-correlated cortical networks of intrinsic BOLD connectivity in the rat brain, in which the midline “DMN-like” cingulate/prefrontal system was inversely coupled to a lateral secondary sensorimotor system.

The anti-correlated networks we observed bear a striking resemblance to anatomical features of anti-correlated human intrinsic connectivity networks. In humans, the DMN is anti-correlated with a set of brain regions that include the supplementary motor area, extending along the precentral gyrus to the frontal eye fields, secondary sensory cortex, and insula (Fox et al., 2005). Our observed lateral cortical network in the rat, anti-correlated with midline cingulate/PFC structures and extending back through secondary sensory cortices to the insula, is highly consistent with the temporal and anatomical features of this part of the human

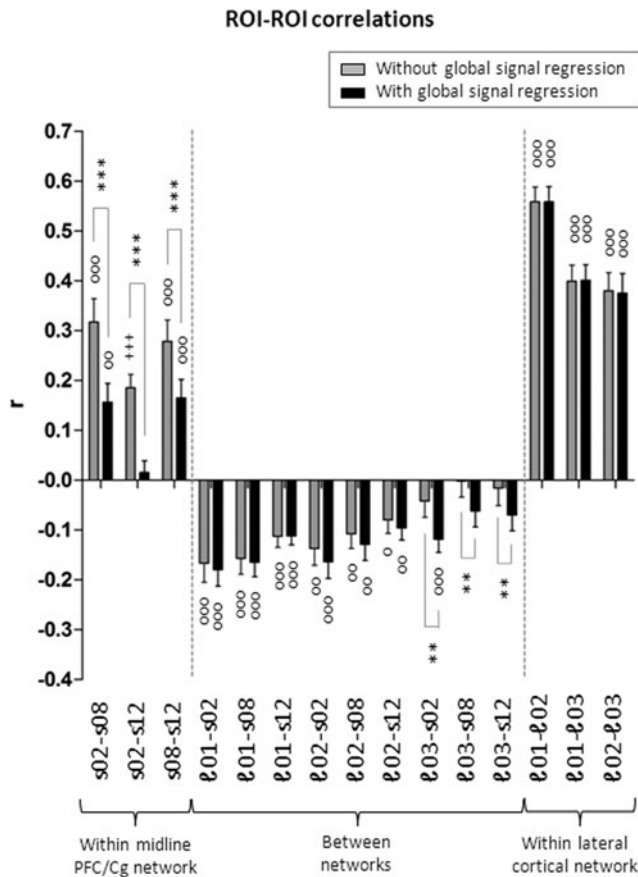


FIG. 3. ROI-ROI correlation relationships within and between networks. The addition of global signal correction (black bars) reduces the correlations between the midline ROIs but does not substantially alter most correlations within the lateral network nor the anti-correlations between networks. Circles denote correlations that are significantly different from zero at the group level ($^{\circ}p < 0.05$; $^{\circ\circ}p < 0.01$; $^{\circ\circ\circ}p < 0.001$; only those surviving false discovery rate correction at $q = 0.05$ are shown). Asterisks denote significant differences between results with and without global signal removal ($*p < 0.05$; $**p < 0.01$; $***p < 0.001$; only those surviving false discovery rate correction at $q = 0.05$ are shown). ROI, regions of interest.

network. Lateral anterior cortical regions in the rat brain, located in the M2 region (Paxinos terminology, as used in this article), are considered to play an integrative role with regard to gaze and orientation and are referred to as frontal orientation fields homologous to frontal eye fields in primates (Erlich et al., 2011). This correspondence further underscores the inter-species homotopy of these lateral cortical networks; indeed, the observed intrinsic connectivity patterns provide an anatomical guide for further exploration of the functional role of these systems in the rat brain via lesion or probe based behavioral studies.

However, in the human, this network also includes regions of the lateral parietal cortex centered on the intraparietal sulcus; we did not observe a clear analogue to this feature in the rat, although posteriorly the lateral network also included weak bilateral foci in the visual cortex (approximate coordinates: LR±2.3, DV 1.2, AP−8.0). This discrepancy

may reflect the increased differentiation of the parietal cortex in primates with regard to the rodent. Other regions within the parietal cortex were coupled to the midline cingulate/retrosplenial cortex network, as observed in the human DMN and previously described in the rat (Lu et al., 2012; Schwarz et al., 2013).

The insular involvement in the rat’s lateral cortical network was primarily restricted to the granular and dysgranular insular cortex between (approximately) $-1.6 \text{ mm} < Z_{\text{bregma}} < 0.8 \text{ mm}$ as well as the more ventral posterior agranular insular cortex in this range. The more rostral dorsal and ventral portions of the agranular insula seemed not to be a part of the lateral cortical network, which involved progressively more dorsolateral brain regions (lateral sensorimotor) toward the anterior aspect of the rat brain. This is consistent with tract tracing studies in which more posterior parts of the rat insular cortex project to lateral rostro-cortical areas (Yasui et al., 1991), in contrast to more rostral regions of the insula that are more strongly connected with ventromedial areas of the rostral cortex (Krushel and van der Kooy, 1988, Yasui et al., 1991).

A previous study of anti-correlated BOLD connectivity features in the rat brain (Liang et al., 2012) reported an anti-correlation relationship between the amygdala and infralimbic cortex, a well-characterized frontolimbic circuit involved in the regulation of emotion and affective behaviors. However, the clear inverse cortico-cortical coupling between midline cingulate/prefrontal structures and the lateral sensorimotor/insula cortical network reported here has not previously been described. The current article thus extends the evidence for anti-correlated functional connectivity involving plausible brain circuits in the rat brain. The anti-correlation relationship reported here was most strongly observed and clearly identified in relation to the anterior secondary motor cortex seed. Moreover, the lateral M2/S2/Ins network was relatively homogeneous—seeds in three locations throughout this network resulted in very similar correlation maps. In contrast, as previously characterized in detail (Schwarz et al., 2013), the midline cingulate and prefrontal seeds revealed more heterogeneous correlation relationships within the larger hippocampal-prefrontal system.

Importantly, our anti-correlation relationships were observed in the absence of global signal correction, suggesting that the anti-correlations *per se* are not simply mathematical artefacts of global signal removal, but a robust feature of functional connectivity in the rat brain. This is consistent with recent advances in human rsfMRI, where the anti-correlated signals originally detected after global signal correction (Fox et al., 2005) have recently been confirmed *in vivo* without this processing step (Chai et al., 2012, Whitfield-Gabrieli and Nieto-Castanon, 2012), demonstrating that robust accounting for possible physiological confounds recovers much of the anti-correlation relationships observed with global signal correction without introducing mathematical confounds (Chang and Glover, 2009; Murphy et al., 2009). The human anti-correlation signature is also supported by electrophysiological evidence that BOLD anti-correlations are closely coupled to anti-correlated gamma band oscillations (Keller et al., 2013).

In the present study, we found largely convergent correlation and anti-correlation relationships when the additional global signal regression step was applied to the data. Correlations within the lateral secondary cortical network were unchanged, and anti-correlations between the two networks

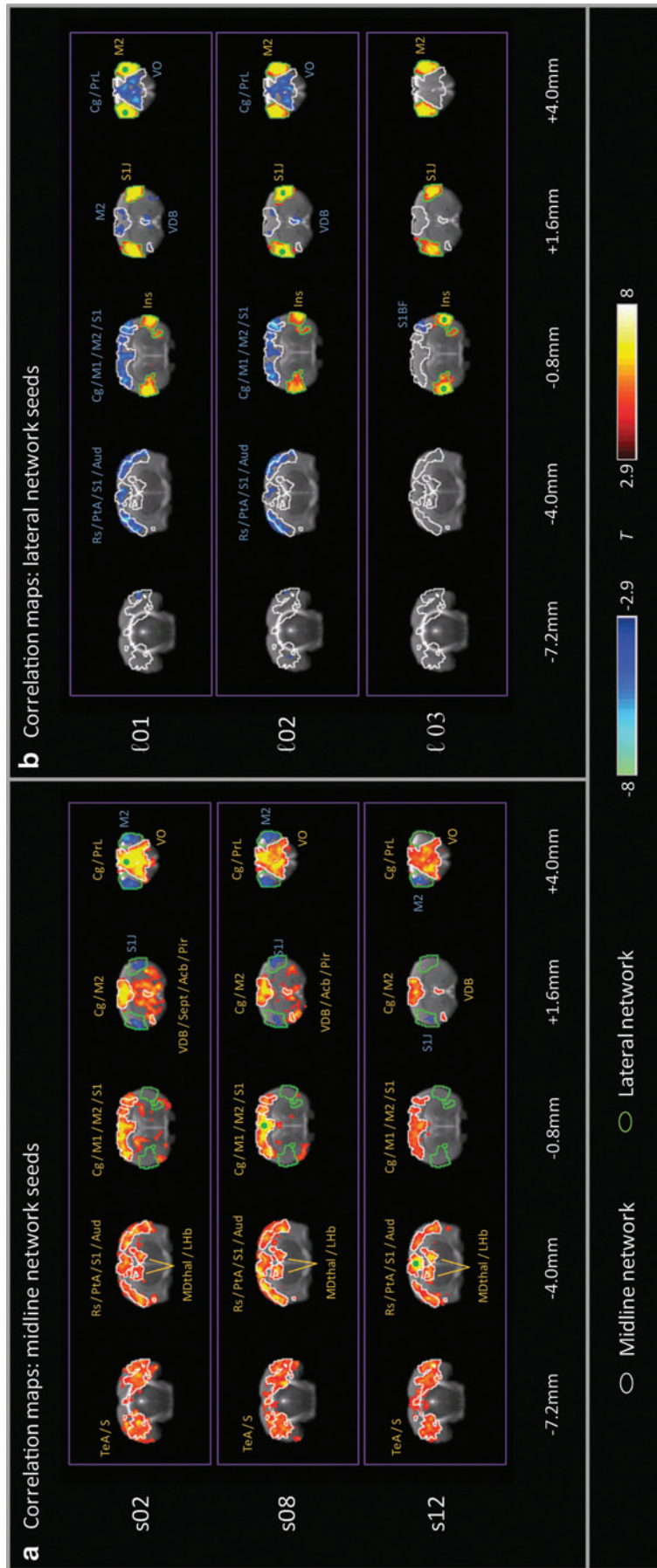


FIG. 4. Seed correlation maps showing positive (red) and negative (blue) correlations ($|T| > 2.9$, $p_{\text{cluster}} < 0.05$) for individual seeds within (a) the midline cingulate/PFC network and (b) lateral secondary cortical network. The white and yellow outlines delineate the overlap in positive correlations across all three seeds in the midline and lateral networks, respectively. Green dots denote seed location for each map. Slice positions denoted A-P relative to bregma.

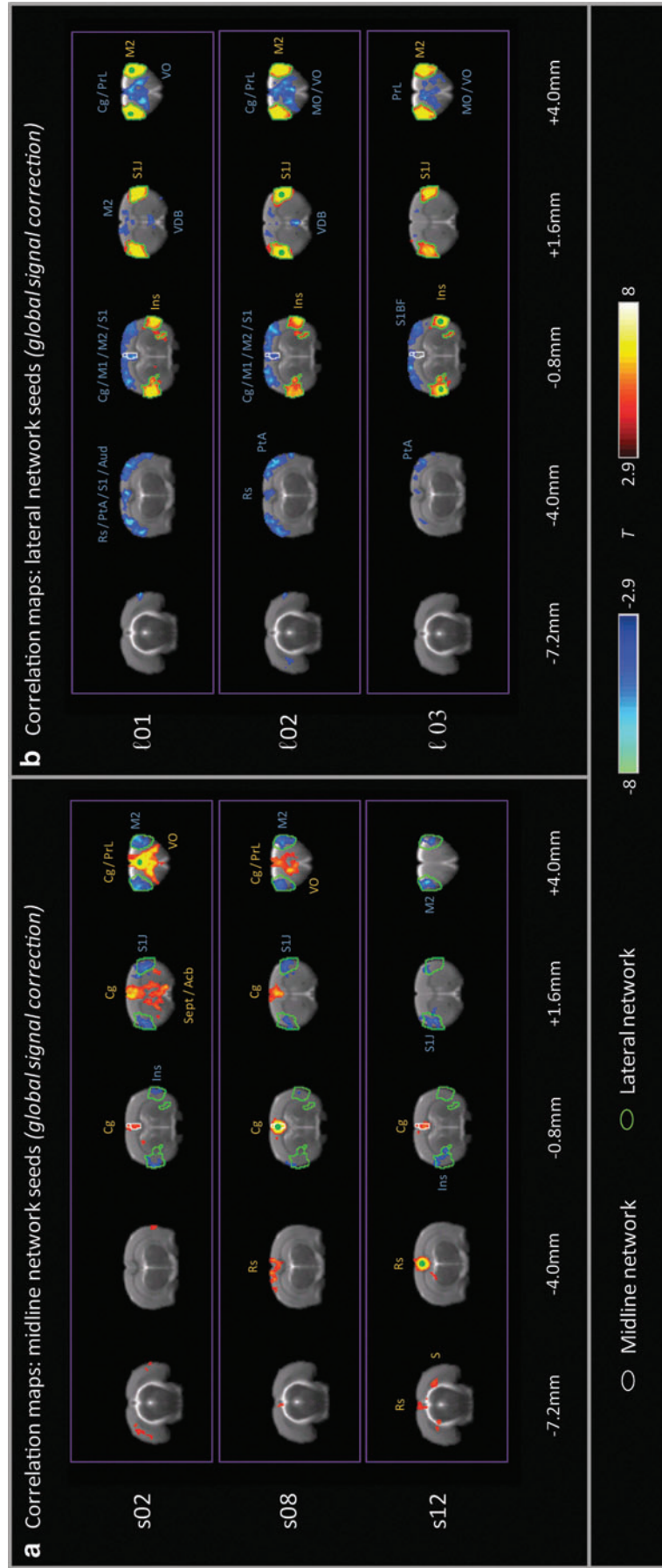


FIG. 5. Seed correlation maps showing positive (red) and negative (blue) correlations ($|T| > 2.9$, $p_{\text{cluster}} < 0.05$) after global signal removal for individual seeds within (a) the midline cingulate/PFC network and (b) lateral secondary cortical network. The white and yellow outlines delineate the overlap in positive correlations across all three seeds in the midline and lateral networks, respectively. Green dots denote seed location for each map. Slice positions denoted A-P relative to bregma.

were similar or slightly stronger. However, correlations within the midline PFC network became more focal after global signal removal, and significantly reduced in the ROI-ROI analysis. This was especially the case for the correlation between the seed in the retrosplenial cortex and that in the anterior prefrontal cortex, which were no longer correlated after global signal correction ($r=0.02$ vs. $r=0.19$). This provides further evidence of the existence of a nontrivial connectivity structure within the midline “DMN-like” network in the rat brain, and warrants further investigation. Although functional connectivity maps associated with these seeds were previously shown to closely mirror known anatomical connectivity within the hippocampal–prefrontal system (Schwarz et al., 2013), potential methodological factors that might preferentially impact this network should be explored. These include potential contamination from signals in the sagittal sinus vein and signal intensity inhomogeneities arising from the use of a surface coil for signal reception.

This article extends the parallels between rat and human rsfMRI findings, replicating in the rat one of the cardinal features of human functional connectivity—the existence of anti-correlated cortical networks—with striking anatomical homology. The extent to which these networks have “task-positive” and “task-negative” behavior in the rat brain, as established in humans, remains unresolved but may be tractable via studies using probe-based or tethered measurements of brain function in the awake, behaving state (Lowry et al., 2010; Schiffer et al., 2007).

Conclusions

We demonstrated the existence of a lateral cortical network of low-frequency BOLD oscillations in the rat brain, extending from anterior secondary sensorimotor regions to the insular cortex, anti-correlated with the midline cingulate/prefrontal network in the rat. This replicates one of the cardinal features of human functional connectivity, and demonstrates a strong anatomical homology with the anterior components of the human “task-positive” network, including consistent involvement of frontal eye field and lateral sensorimotor cortical regions across species. These relationships were observed after RETROICOR-type postprocessing and corroborated after global signal removal, suggesting that they are a robust feature of rat brain functional organization and further the extent to which connectivity features observed in primates have been demonstrated to be preserved in rodents. This supports the use of resting-state fMRI as a translatable imaging method between rat models and humans.

Acknowledgments

The research leading to these results has received support from the Innovative Medicine Initiative Joint Undertaking under Grant Agreement No. 115008 (NEWMEDS) of which resources are composed of European Federation of Pharmaceutical Industries and Associations (EFPIA) in-kind contribution and financial contribution from the European Union’s Seventh Framework Program (FP7/2007–2013). This work was also partially funded through a grant from the German Ministry of Education and Research (BMBF, 01GQ1003B).

Author Disclosure Statement

AJS is an employee and shareholder of Eli Lilly and Company. CR is an employee of F. Hoffman La Roche Ltd. ES and MS are employees of Institut de Recherche Servier.

References

- Ashburner J. 2011. SPM: A history. *Neuroimage* 62:791–800.
- Beckmann CF, DeLuca M, Devlin JT, Smith SM. 2005. Investigations into resting-state connectivity using independent component analysis. *Philos Trans R Soc Lond B Biol Sci* 360: 1001–1013.
- Biswal B, Yetkin FZ, Haughton VM, Hyde JS. 1995. Functional connectivity in the motor cortex of resting human brain using echo-planar MRI. *Magn Reson Med* 34:537–541.
- Chai XJ, Castanon AN, Ongur D, Whitfield-Gabrieli S. 2012. Anticorrelations in resting state networks without global signal regression. *Neuroimage* 59:1420–1428.
- Chang C, Glover GH. 2009. Effects of model-based physiological noise correction on default mode network anti-correlations and correlations. *Neuroimage* 47:1448–1459.
- Cox RW. 2012. AFNI: What a long strange trip it’s been. *Neuroimage* 62:743–747.
- Erlich JC, Bialek M, Brody CD. 2011. A cortical substrate for memory-guided orienting in the rat. *Neuron* 72:330–343.
- Fox MD, Raichle ME. 2007. Spontaneous fluctuations in brain activity observed with functional magnetic resonance imaging. *Nat Rev Neurosci* 8:700–711.
- Fox MD, Snyder AZ, Vincent JL, Corbetta M, Van Essen DC, Raichle ME. 2005. The human brain is intrinsically organized into dynamic, anticorrelated functional networks. *Proc Natl Acad Sci U S A* 102:9673–9678.
- Gass N, Schwarz AJ, Sartorius A, Cleppien D, Zheng L, Schenker E, Risterucci C, Meyer-Lindenberg A, Weber-Fahr W. 2013. Haloperidol modulates midbrain-prefrontal functional connectivity in the rat brain. *Eur Neuropsychopharmacol*. [Epub ahead of print]; DOI: 10.1016/j.euroneuro.2012.10.013.
- Glover GH, Li TQ, Ress D. 2000. Image-based method for retrospective correction of physiological motion effects in fMRI: RETROICOR. *Magn Reson Med* 44:162–167.
- Hutchison RM, Everling S. 2012. Monkey in the middle: why non-human primates are needed to bridge the gap in resting-state investigations. *Front Neuroanat* 6:29.
- Jenkinson M, Beckmann CF, Behrens TE, Woolrich MW, Smith SM. 2012. Fsl. *Neuroimage* 62:782–790.
- Jonckers E, Van Audekerke J, De Visscher G, Van der Linden A, Verhoye M. 2011. Functional connectivity fMRI of the rodent brain: comparison of functional connectivity networks in rat and mouse. *PLoS One* 6:e18876.
- Keller CJ, Bickel S, Honey CJ, Groppe DM, Entz L, Craddock RC, Lado FA, Kelly C, Milham M, Mehta AD. 2013. Neurophysiological Investigation of Spontaneous Correlated and Anticorrelated Fluctuations of the BOLD Signal. *J Neurosci* 33:6333–6342.
- Krushel LA, van der Kooy D. 1988. Visceral cortex: integration of the mucosal senses with limbic information in the rat agranular insular cortex. *J Comp Neurol* 270:39–54, 62–33.
- Liang Z, King J, Zhang N. 2012. Anticorrelated resting-state functional connectivity in awake rat brain. *Neuroimage* 59:1190–1199.
- Lowry JP, Griffin K, McHugh SB, Lowe AS, Tricklebank M, Sibson NR. 2010. Real-time electrochemical monitoring of brain tissue oxygen: a surrogate for functional magnetic resonance imaging in rodents. *Neuroimage* 52:549–555.

- Lu H, Zou Q, Gu H, Raichle ME, Stein EA, Yang Y. 2012. Rat brains also have a default mode network. *Proc Natl Acad Sci U S A* 109:3979–3984.
- Murphy K, Birn RM, Handwerker DA, Jones TB, Bandettini PA. 2009. The impact of global signal regression on resting state correlations: are anti-correlated networks introduced? *Neuroimage* 44:893–905.
- Nasrallah FA, Tan J, Chuang KH. 2012. Pharmacological modulation of functional connectivity: alpha2-adrenergic receptor agonist alters synchrony but not neural activation. *Neuroimage* 60:436–446.
- Pawela CP, Biswal BB, Cho YR, Kao DS, Li R, Jones SR, Schulte ML, Matloub HS, Hudetz AG, Hyde JS. 2008. Resting-state functional connectivity of the rat brain. *Magn Reson Med* 59:1021–1029.
- Paxinos G, Watson C. 1998. *The Rat Brain in Stereotaxic Coordinates*. San Diego: Academic Press.
- Raichle ME. 2011. The restless brain. *Brain Connect* 1:3–12.
- Raichle ME, MacLeod AM, Snyder AZ, Powers WJ, Gusnard DA, Shulman GL. 2001. A default mode of brain function. *Proc Natl Acad Sci U S A* 98:676–682.
- Schiffer WK, Mirrione MM, Dewey SL. 2007. Optimizing experimental protocols for quantitative behavioral imaging with 18F-FDG in rodents. *J Nucl Med* 48:277–287.
- Schwarz AJ, Danckaert A, Reese T, Gozzi A, Paxinos G, Watson C, Merlo-Pich EV, Bifone A. 2006. A stereotaxic MRI template set for the rat brain with tissue class distribution maps and co-registered anatomical atlas: application to pharmacological MRI. *Neuroimage* 32:538–550.
- Schwarz AJ, Gass N, Sartorius A, Zheng L, Spedding M, Schenker E, Risterucci C, Meyer-Lindenberg A, Weber-Fahr W. 2013. The low-frequency blood oxygenation level-dependent functional connectivity signature of the hippocampal-prefrontal network in the rat brain. *Neuroscience* 228:243–258.
- Upadhyay J, Baker SJ, Chandran P, Miller L, Lee Y, Marek GJ, Sakoglu U, Chin CL, Luo F, Fox GB, Day M. 2011. Default-mode-like network activation in awake rodents. *PLoS One* 6:e27839.
- van Buuren M, Gladwin TE, Zandbelt BB, van den Heuvel M, Ramsey NF, Kahn RS, Vink M. 2009. Cardiorespiratory effects on default-mode network activity as measured with fMRI. *Hum Brain Mapp* 30:3031–3042.
- Vincent JL, Patel GH, Fox MD, Snyder AZ, Baker JT, Van Essen DC, Zempel JM, Snyder LH, Corbetta M, Raichle ME. 2007. Intrinsic functional architecture in the anaesthetized monkey brain. *Nature* 447:83–86.
- Whitfield-Gabrieli S, Nieto-Castanon A. 2012. Conn: a functional connectivity toolbox for correlated and anticorrelated brain networks. *Brain Connect* 2:125–141.
- Yasui Y, Breder CD, Saper CB, Cechetto DF. 1991. Autonomic responses and efferent pathways from the insular cortex in the rat. *J Comp Neurol* 303:355–374.
- Zhang N, Rane P, Huang W, Liang Z, Kennedy D, Frazier JA, King J. 2010. Mapping resting-state brain networks in conscious animals. *J Neurosci Methods* 189:186–196.

Address correspondence to:
Adam J. Schwarz
Eli Lilly and Company
Lilly Corporate Center
DC 1940
Indianapolis, IN 46285

E-mail: a.schwarz@lilly.com